UNIVERSITYOF BIRMINGHAM

Sensors and Actuators for the Advanced LIGO+ Upgrade

Cooper, S J; Mow-Lowry, C M; Hoyland, D; Bryant, J; Ubhi, A; O'Dell, J; Huddart, A; Aston, S; Vecchio, A

[Link to publication on Research at Birmingham portal](#)

Sensors and Actuators for the Advanced LIGO+ Upgrade

S J Cooper,[1] C M Mow-Lowry,[1, *] D Hoyland,[1] J Bryant,[1]
A Ubhi,[1] J O'Dell,[2] A Huddart,[2] S Aston,[3] and A Vecchio[1, †]

[1]*Institute for Gravitational Wave Astronomy & School of Physics and
Astronomy, University of Birmingham, Birmingham, B15 2TT, UK*
[2]*Science and Technology Facilities Council, Rutherford Appleton Laboratory, Harwell Campus, Didcot, OX11 0QX, UK*
[3]*LIGO Livingston Observatory, Livingston, LA 70754, United States of America*
(Dated: August 2, 2022)

As part of the Advanced LIGO+ (A+) project we have developed, produced, and characterised sensors and electronics to interrogate new optical suspensions. The central element is a displacement sensor with an integrated electromagnetic actuator known as a BOSEM and its readout and drive electronics required to integrate them into LIGO's control and data system. In this paper we report on improvements to the sensors and testing procedures undertaken to meet enhanced performance requirements set out by the A+ upgrade to the detectors. The best devices reach a noise level of 4.5×10^{-11} m/$\sqrt{\text{Hz}}$ at a measurement frequency of 1 Hz.

I. INTRODUCTION

The Advanced LIGO [1] and Virgo [2] gravitational-wave interferometers have opened explorations of the gravitational-wave sky, with the observation of the coalescence of stellar-mass binary black holes [3–8], binary neutron stars [9–11] and more recently neutron star-black hole systems [12].

The LIGO and Virgo detectors are being upgraded to what is known as 'Advanced+' (A+, hereafter) configuration. Installation has already begun for some of the hardware. After the forth observing run (O4) scheduled to start in 2022, it will be completed in advance of the fifth observing run in 2025 [13]. The higher sensitivity achieved through this upgrade will correspond to an increase of the Universe's observable volume by a factor ≈ 5 with respect to the one probed by the existing instruments, resulting in an equal increase in detection rate. For example, based on current estimates of the merger rate of populations of stellar-mass binary systems [14] and the expected instrument performance in A+ configurations, the detectors will observe several of such binary coalescences every week, *e.g.* [15].

LIGO A+ will achieve this increase in observing range by upgrading several sub-systems of the detectors: new test-masses with reduced coating thermal noise [16], frequency-dependent squeezing [17], replacement the central beam-splitter with a larger optic, and installation of balanced homodyne detection [18] to further reduce quantum noise.

These upgrades will require several new multi-stage suspension systems for isolating and controlling the new optical elements. Each suspension requires a set of low-noise sensors and actuators, with associated electronics, to actively damp resonances and steer the laser beam. One example of a new suspension, shown in Fig. 1, is the 'HAM Relay Triple Suspension', an evolution of existing suspension designs that is lighter and easier to assemble. In total, 200 BOSEMs – "Birmingham Optical Sensor and Electro-Magnetic actuator" – have been produced, along with 82 coil-driver units and 44 'satellite amplifiers' for reading out the photocurrent.

This paper updates the design produced for Advanced LIGO [19, 20] to fulfil existing and enhanced sensitivity requirements for A+. A noise budget with the dominant terms is provided, with reference to the exhaustive selection procedure required. More than half of the BOSEMs reach a new 'Enhanced' performance requirement. The best Enhanced BOSEMs are now dominated by quantum shot noise across the whole measurement band, a major performance improvement.
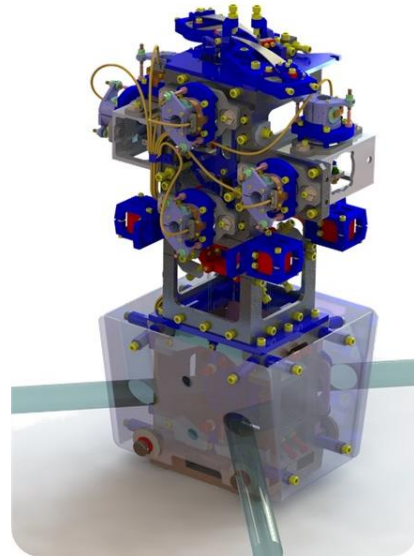

FIG. 1. A rendered image of the new HAM Relay Tiple Suspension with BOSEMs installed.

* Now at the Vrije Universiteit Amsterdam
† av@star.sr.bham.ac.uk

II.   BOSEM DESIGN

BOSEMs are compact, ultra-high vacuum compliant, non-contact, and low-noise position sensors with integrated electromagnetic actuators. They have a long history of development started by studies on the initial LIGO OSEMS by Fritschel [21], which were upgraded to AOSEMS by Abbott [22] and modified by Carbone [19] to produce the Advanced LIGO BOSEMs. A table of key parameters for each BOSEM can be found in Table I.

Each BOSEM unit comprises of a number of elements: sensing, actuation, and alignment. An exploded CAD model of the BOSEM is shown in Fig. 2, with key features of the sensor labelled. The optical readout is based on a shadow sensing scheme where an opaque 'flag', rigidly mounted to the measurement surface [23], partly blocks 935 nm light emitted from an Infra-Red LED (IRLED, Optek OP132) before it is sensed by a photodiode (PD, Osram BPX65). The choice of wavelength ensures high quantum efficiency from the silicon photodiode and negligible emission at 1064 m, the wavelength of the main science laser. A lens is installed after the LED to produce a narrower beam and smaller spot on the photodiode, improving both the linearity and sensitivity of the BOSEM.
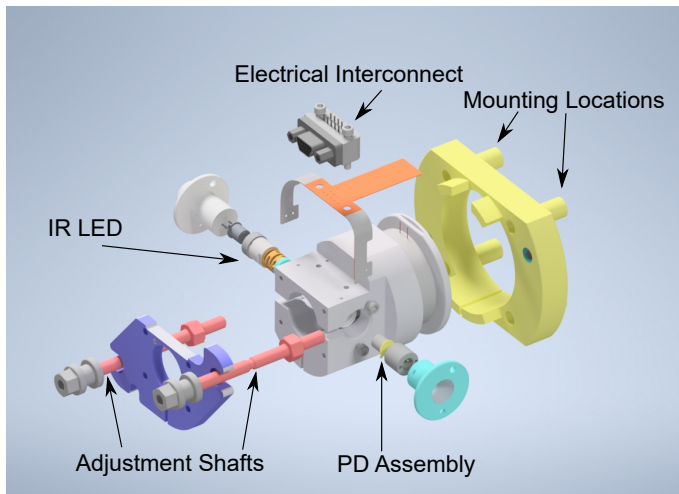

FIG. 2. An exploded view of a BOSEM highlighting key components.

To meet LIGO's stringent vacuum requirements, the BOSEMs must go through a multi-stage cleaning process. In the original production run toluene was used in the cleaning process to remove paraffin from the coil wire [24]. Following the detection of toluene residue in RGA scans during the production process the coil wire was switched(from MWS Wire 32 HML to MWS Wire 32 HML Natural) to ensure the production process was paraffin-free. The updated cleaning process can be found in [25].

TABLE I. Key parameters for a BOSEM.

Parameter	Value
Coil	
Turns	800
Winding sense	Clockwise when viewed from the rear face
Inductance	$14.7 \pm 0.7\,\mathrm{mH}$
Resistance	$37.6 \pm 2\,\Omega$
Length	$8\,\mathrm{mm}$
Inner coil diameter	$17.8\,\mathrm{mm}$
Maximum current	$150\,\mathrm{mA}$
Breakdown (to coil former)	$>200\,\mathrm{V}$
Sensor	
Mass	$158\,\mathrm{g}$
Linear range (typ.)	$0.7\,\mathrm{mm}$
Operating LED current	$35\,\mathrm{mA}$
Photodiode bias	10 V typ. (50 V max.)
Photocurrent, open-light	$45\text{-}80\,\mu\mathrm{A}$
Current transfer ratio	$0.19 \pm 0.04\%$
Average sensitivity	$20.25\,\mathrm{kV/m}$
Electrical connector	Glenair micro-D MR7590-9P-1BSN-MC225
Mechanical Interface	4x 8/32UNC thru-holes on 40.64 mm (1.3") square grid
Operating temperature	$22 \pm 2^\circ$ C
Storage temperature (ambient pressure)	10 to 120°C
Sensor Noise	
Standard	
1-10 Hz	$3\mathrm{x}10^{-10}\,\mathrm{m}/\sqrt{\mathrm{Hz}}$
10-20 Hz	$1\mathrm{x}10^{-10}\,\mathrm{m}/\sqrt{\mathrm{Hz}}$
Enhanced	
1-20 Hz	$<0.75\mathrm{x}10^{-10}\,\mathrm{m}/\sqrt{\mathrm{Hz}}$

III.   PERFORMANCE ANALYSIS

The noise budget of a BOSEM is shown in Fig. 3. The noise sources expected to dominate a typical system are the shot noise and the photodiode dark noise. The shot noise, shown in dark blue, is modelled and projected to an equivalent displacement using

$$SN = \frac{2R}{K}\sqrt{2eI} \tag{1}$$

where e is the electronic charge, I is the photocurrent at the operating point (the 'half-light' current), R is the transimpedance gain of $121\,\mathrm{k\Omega}$, and K is the sensivity of the BOSEM which varies depending on the photocurrent but averages 20250 volts per metre. The leading factor of 2 accounts for the differential output gain of the satellite amplifier. The photodiode dark noise, shown in red, was measured by switching off the IRLED and measuring the
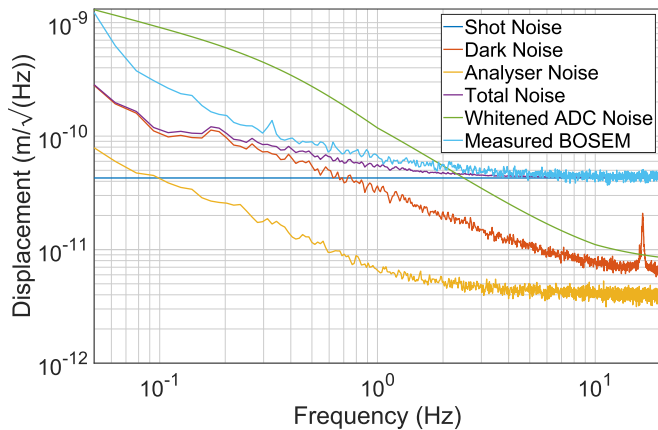
FIG. 3. A noise budget of an Enhanced BOSEM showing each of the individual noise contributions. The main noise sources are the shot noise (dark blue) and the photodiode dark noise (red). The resolution of the BOSEM at the critical 10 Hz measurement frequency is limited by optical shot noise.
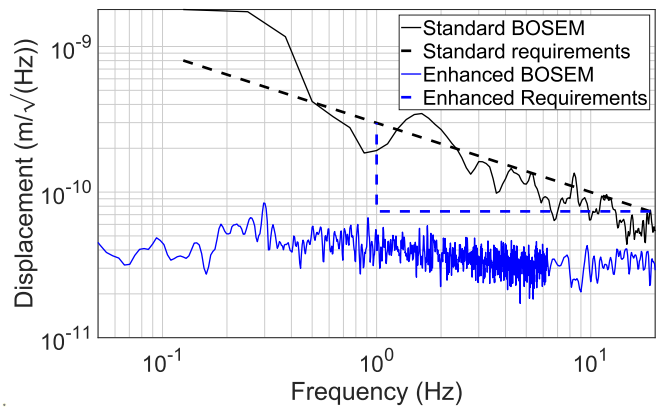

FIG. 4. Amplitude Spectral density of the Standard (black) and Enhanced (blue) BOSEMs compared against the noise requirements shown with dashed lines.

output of the satellite amplifier [19].

The total modelled noise trace, shown in purple, is achieved by summing the shot noise and dark noise in quadrature. The noise model is compared with the spectrum of a typical BOSEM 'open light test', where there is no flag inserted in the beam, shown in light blue. Since the open light test has a factor of 2 more photocurrent than normal half-light operation, to calibrate it into metres we divide by a factor of $\sqrt{2}$ before using the volts-to-metres conversion factor. This will correctly scale the shot-noise for the photocurrent expected under normal operating conditions.

The noise floor of our signal analyser is shown for reference in yellow. The whitened ADC noise of LIGO's Control and Data System is shown in green; at frequencies lower than 1 Hz we expect BOSEMs installed at LIGO to be dominated by this noise source.

There is a clear discrepancy between the noise model and the measurement of a typical BOSEM. Two contributions have been identified. First, the photodiode dark noise varies from unit to unit, presumably due to defects in individual photodiodes. Repeated measurements have shown that this never exceeds the noise requirements and to be sub-dominant in almost all BOSEM assemblies. Second, the IRLEDs show significant excess intensity fluctuation, and this is the dominant source of excess noise. This excess noise was identified in the original Advanced LIGO BOSEM production run and a screening process was implemented to select IRLEDs that comply with the noise requirements [26]. For the A+ upgrade we conducted an extensive review of different IRLEDs, but no model was shown to consistently meet the noise requirements. Instead, the Advanced LIGO screening process was improved, most importantly by lengthening the initial 'burn in' from 50 hours to 168 hours as detailed in [27].

To capitalise on the effort involved in screening every IRLED, we identified units with especially good noise performance between 1 Hz and 20 Hz. If these units met a new 'Enhanced' noise requirement they were separated and tagged for use in critical locations. They do not require any change to the existing signal chain. Figure 4 shows the noise spectra of a Standard BOSEM and an Enhanced BOSEM, along with their respective requirements. The best of the Enhanced BOSEMs are dominated by shot noise across the whole measurement band. Further improvements can come from reducing the measurement range (increasing sensitivity), for example the Differential-OSEM sensors [28], or by using alternative technology such as fringe-counting interferometers [29], which have improved resolution without sacrificing operating range.

IV. CONCLUSIONS

As part of the Advanced LIGO+ upgrade the University of Birmingham has provided over 200 BOSEM sensors and actuators along with their associated driving electronics. Over half of the BOSEMs meet the 'Enhanced' specification. The best units have a resolution of $4.5\times10^{-11}\,\mathrm{m}\sqrt{\mathrm{Hz}}$ all the way down to 0.1 Hz and these devices represent the ultimate performance of BOSEMs in their current form.

ACKNOWLEDGMENTS

[1] A. Buikema et al. Sensitivity and performance of the Advanced LIGO detectors in the third observing run. *Phys. Rev. D*, 102:062003, 2020.

[2] F. Acernese, M. Agathos, A. Ain, S. Albanesi, A. Allocca, A. Amato, T. Andrade, N. Andres, T. Andrić, S. Ansoldi, et al. Calibration of advanced virgo and reconstruction of detector strain h(t) during the observing run O3. *arXiv preprint arXiv:2107.03294*, 2021.

[3] B.P. Abbott et al. Observation of Gravitational Waves from a Binary Black Hole Merger. *Phys. Rev. Lett.*, 116(6):061102, 2016.

[4] B.P. Abbott et al. Binary Black Hole Mergers in the first Advanced LIGO Observing Run. *Phys. Rev. X*, 6(4):041015, 2016. [Erratum: Phys.Rev.X 8, 039903 (2018)].

[5] B.P. Abbott et al. GWTC-1: A Gravitational-Wave Transient Catalog of Compact Binary Mergers Observed by LIGO and Virgo during the First and Second Observing Runs. *Phys. Rev. X*, 9(3):031040, 2019.

[6] R. Abbott et al. GWTC-2: Compact Binary Coalescences Observed by LIGO and Virgo During the First Half of the Third Observing Run. *Phys. Rev. X*, 11:021053, 2021.

[7] R. Abbott et al. GWTC-2.1: Deep Extended Catalog of Compact Binary Coalescences Observed by LIGO and Virgo During the First Half of the Third Observing Run. 8 2021.

[8] R. Abbott et al. GWTC-3: Compact Binary Coalescences Observed by LIGO and Virgo During the Second Part of the Third Observing Run. 11 2021.

[9] B.P. Abbott et al. GW170817: Observation of Gravitational Waves from a Binary Neutron Star Inspiral. *Phys. Rev. Lett.*, 119(16):161101, 2017.

[10] B.P. Abbott et al. Multi-messenger Observations of a Binary Neutron Star Merger. *Astrophys. J. Lett.*, 848(2):L12, 2017.

[11] B.P. Abbott et al. GW190425: Observation of a Compact Binary Coalescence with Total Mass $\sim 3.4 M_\odot$. *Astrophys. J. Lett.*, 892:L3, 2020.

[12] R. Abbott et al. Observation of gravitational waves from two neutron star-black hole coalescences. *Astrophys. J. Lett.*, 915:L5, 2021.

[13] B.P. Abbott et al. Prospects for Observing and Localizing Gravitational-Wave Transients with Advanced LIGO, Advanced Virgo and KAGRA. *Living Rev. Rel.*, 21(1):3, 2018.

[14] R. Abbott et al. The population of merging compact binaries inferred using gravitational waves through GWTC-3. 11 2021.

[15] J. Miller, L. Barsotti, S. Vitale, P. Fritschel, M. Evans, and D. Sigg. Prospects for doubling the range of Advanced LIGO. *Phys. Rev. D*, 91:062005, 2015.

[16] M. Abernathy, A. Amato, A. Ananyeva, S. Angelova, B. Baloukas, R. Bassiri, G. Billingsley, R. Birney, G. Cagnoli, M. Canepa, et al. Exploration of co-sputtered Ta_2O_5-ZrO_2 thin films for gravitational-wave detectors. *arXiv preprint arXiv:2103.14140*, 2021.

[17] L. McCuller, C. Whittle, D. Ganapathy, K. Komori, M. Tse, A. Fernandez-Galiana, L. Barsotti, P. Fritschel, M. MacInnis, F. Matichard, K. Mason, N. Mavalvala, R. Mittleman, Haocun Yu, M. E. Zucker, and M. Evans. Frequency-dependent squeezing for Advanced LIGO. *Phys. Rev. Lett.*, 124:171102, 2020.

[18] P. Fritschel, M. Evans, and V. Frolov. Balanced homodyne readout for quantum limited gravitational wave detectors. *Opt. Express*, 22:4224–4234, 2014.

[19] L. Carbone, S. M. Aston, R. M. Cutler, A. Freise, J. Greenhalgh, J. Heefner, D. Hoyland, N. A. Lockerbie, D. Lodhia, N. A. Robertson, C. C. Speake, K. A. Strain, and A. Vecchio. Sensors and actuators for the advanced LIGO mirror suspensions. *Classical and Quantum Gravity*, 29:115005, 2012.

[20] S M Aston, M A Barton, A S Bell, N Beveridge, B Bland, A J Brummitt, G Cagnoli, C A Cantley, L Carbone, A V Cumming, L Cunningham, R M Cutler, R J S Greenhalgh, G D Hammond, K Haughian, T M Hayler, A Heptonstall, J Heefner, D Hoyland, J Hough, R Jones, J S Kissel, R Kumar, N A Lockerbie, D Lodhia, I W Martin, P G Murray, J O'Dell, M V Plissi, S Reid, J Romie, N A Robertson, S Rowan, B Shapiro, C C Speake, K A Strain, K V Tokmakov, C Torrie, A A van Veggel, A Vecchio, and I Wilmut. Update on quadruple suspension design for advanced LIGO. *Classical and Quantum Gravity*, 29:235004, 2012.

[21] P. Fritschel and R. Adhikari. Characterization and comparison of a potential new (sus) local sensor. *LIGO Document Control Center*, 2015. Available at `https://dcc.ligo.org/LIGO-T990089/public`.

[22] R. Abbott, M. Barton, B. Bland, B. Moore, C. Osthelder, and J. Romie. Advanced LIGO OSEM final design document. *LIGO Document Control Center*, 2014. Available at `https://dcc.ligo.org/LIGO-T0900286/public`.

[23] M. Evans and M. Hillard. BOSEM flat magnet flag, aLIGO SUS. *LIGO Document Control Center*, 2011. Available at `https://dcc.ligo.org/LIGO-D1100573/public`.

[24] C. Taylor. Cleaning procedure for magnet wire with ML/HML insulation. *LIGO Document Control Center*, 2019. Available at `https://dcc.ligo.org/T040127`.

[25] J.L. Bryant S. M. Aston, D. Lodhia and D. Hoyland. BOSEM assembly specification. *LIGO Document Control Center*, 2021. Available at `https://dcc.ligo.org/LIGO-T060233/public`.

[26] S. M. Aston. *Optical read-out techniques for the control of test-masses in gravitational wave observatories.* University of Birmingham, 2011. Available at `https://etheses.bham.ac.uk/id/eprint/1665/`.

[27] D. Hoyland and J. L. Bryant. A+ BOSEM IR-LED screening. *LIGO Document Control Center*, 2019. Available at `https://dcc.ligo.org/LIGO-T1900596/public`.

[28] J. Conklin, D. Jariwala, T Pechsiri, H. Inchauspe, P. Fulda, and D. Tanner. Progress in developing a

Differential OSEM (DOSEM). *LIGO Document Control Center*, 2019. Available at `https://dcc.ligo.org/LIGO-G1900464`, manuscript in preparation.

[29] S. J. Cooper, C. J. Collins, A. C. Green, D. Hoyland, C. C. Speake, A. Freise, and C. M. Mow-Lowry. A compact, large-range interferometer for precision measurement and inertial sensing. *Classical and Quantum Gravity*, 35:095007, 2018.